Barrier-free liquid condensates of nanocatalysts as effective concentrators of catalysis

Silky Bedi,[a] Gaurav Kumar, [a] S M Rose [a], Sabyasachi Rakshit,*[b] Sharmistha Sinha *[a]

[a] Chemical Biology Unit, Institute of Nano Science and Technology, Sector-81, Knowledge City, Sahibzada Ajit Singh Nagar, Punjab, 140306. E-mail: sinhas@inst.ac.in

[b] Department of Chemical Sciences, Indian Institute of Science Education and Research, Sector-81, Knowledge City, Sahibzada Ajit Singh Nagar, Punjab, 140306. E-mail: srakshit@iisermohali.ac.in

Keywords- Membrane-free Compartmentalization, Liquid-liquid Phase separation, Protein-metal Nanocatalysts, Catalysis.

Experimental

Material and Methods-

All the chemicals unless mentioned are procured from Sigma-Aldrich. Copper chloride dihydrate and sodium sulphate are purchased from HiMedia. Ortho-phenylenediamine (OPD) is procured from TCI chemicals. Construct of α-synuclein is kindly provided by Prof. Samrat Mukhopadhyay, IISER Mohali. All other reagents are of analytical grade and used as received. Ultrapure water is used throughout the experiments.

Synthesis and characterisation of BSA-Au nanocomposites -

We synthesized BSA capped gold nanoclusters (BSA@AuNCs) and BSA capped gold nanoparticles (BSA@AuNPs) according to the method reported by Xie[26] and Matei et al[27] with some modifications. For BSA@AuNCs, 1 ml of 10 mg/ml of dialysed BSA protein solution is mixed with $HAuCl_4$ solution (10mM). The reaction mixture stirred vigorously at 37°C for half an hour followed by the addition of 200µl of 1M NaOH. The reaction is kept stirring for the next 8-10 hours till the development of the dark brown colored solution. Completion of reaction is confirmed by recording the absorption and fluorescence spectra of BSA@AuNCs using Cary UV-Vis compact Peltier spectrophotometer (Agilent, USA) and Spectrofluorimeter FS5 (Edinburgh Instruments, UK) respectively. Prepared Nanoclusters are dialysed using a 3.5 KDa dialysis membrane against distilled water for continuous 48 hours to make the pH of nanoclusters neutral and stored at 4°C for further use. Further, the size of nanoclusters is confirmed using a ZetaSizer Nano ZSP (Malvern Instruments, UK). The scattered intensity is measured at a backscattered angle of 173°. For each sample, three readings are recorded. To understand the morphology of the BSA@AuNCs, TEM images are obtained by drop-casting 10 µl of 0.5 mg/ml nanocluster on glow discharged carbon-coated TEM grids. The grids are then washed with Milli-Q water and a dried using desiccator for 24 hours at room temperature. TEM imaging is done by using JEM 2100 TEM (JEOL, USA) operated at 200 kV.

To prepare BSA@AuNPs, we mixed BSA (5mg/ml) with $HAuCl_4$ solution (100µM). The solution is vigorously stirred at room temperature. To optimize the $NaBH_4$ concentration, various amounts of $NaBH_4$ were added to the solution. The pink-red solution of BSA@AuNPs is prepared using a 1mM concentration of $NaBH_4$. Further, we recorded its UV-Vis absorption spectra using a Cary UV-Vis compact peltier spectrophotometer (Agilent, USA).

Phase separation of BSA-Au nanocomposites-

To visualize the effect of changing ionic strength on BSA and BSA-Au nanocomposites, we performed fluorescence microscopy experiments. We labeled the BSA with TEXAS Red dye and removed the unbound dye by extensive dialysis against water for continuous 48 hours. We prepared samples having 1mg/ml of labelled BSA incubated with increasing sodium sulphate concentration in the range from 50mM-500mM followed by the addition of 5% w/v crowding agent, PEG-6000. Next, we performed the fluorescence microscopic study of BSA@AuNCs and BSA@AuNPs prepared using texas-red labeled BSA. To prepare samples we used 1mg/ml of nanocomposite incubated with sodium sulphate (50-500mM) and 5% w/v of PEG-6000. Prepared samples are drop cast on the microscope slides and visualized using a 10X objective lens in the red channel of Cytation-5 Cell Imaging Multi-Mode Reader (BioTek Instruments).

Co-localisation of protein and gold metal inside liquid droplets-

To check the co-localization of protein and gold metal inside liquid droplets, we designed a scattering-based light-microscopic assay. The design of the experiment is based on the hypothesis that the presence of metal ions in the droplets would scatter more light in comparison to a protein liquid droplet. For this experiment, samples are prepared by incubating 1mg/ml of BSA and BSA@AuNCs with 500mM Na_2SO_4 AND 5%w/v of PEG-6000 differently. The samples having phase separated liquid droplets are drop cast onto the glass coverslip and placed under a 40X objective lens of the inverted fluorescence microscope (IX83 P2ZF Inverted microscope equipped with IX83 MITICO TIRF illuminator). The droplets are excited using the Cy3 channel (excitation wavelength 535 nm) with a laser intensity of 25% at an exposure time of 440 ns. Scattering is collected at Cy3 channel as metal nanoparticles do not emit at this wavelength. To check the change in morphology after phase separation of BSA@AuNCs as liquid condensates, we performed the TEM imaging of phase separated BSA@AuNCs. TEM images are obtained by drop casting 10 µl of the sample having 1mg/ml of BSA@AuNCs mixed with 500mM sodium sulphate and 5% w/v PEG-6000 onto carbon-coated TEM grids. The grids are then washed with Milli-Q water and dried using a desiccator for 24 hours at room temperature. TEM imaging is done by using JEM 2100 TEM (JEOL, USA) operated at 200 kV.

Synthesis of BSA-Copper phosphate nanoflowers-

BSA-Copper phosphate nanoflowers are prepared according to the latest publication from our lab by Kaur et al[28], incubating BSA solution (5µM) with $CuCl_2$ dihydrate (500µM) in phosphate buffer saline pH 7.4. The sample is kept on stirring at room temperature for continuous 24 hours followed by centrifugation of the sample at 10,000rpm for ten minutes. Pellet is extensively washed with water to remove the excess salts. Further, we performed Scanning electron microscopy to confirm the formation and morphology of synthesized BSA-Copper phosphate nanoflowers.

Catalytic activity of BSA-metal nanocomposites-

We checked the catalytic potential of prepared BSA@AuNCs and BSA@AuNPs by performing oxidation and reduction of aromatic compounds in dispersed and phase separated forms. Reduction of p-nitrophenol to p-aminophenol is performed using BSA@AuNCs and BSA@AuNPs in dispersed and phase separated form. The concentration of both systems is normalized by keeping the concentration of BSA constant. 1mg/ml of BSA@AuNCs and BSA@AuNPs is mixed with 100µM of p-nitrophenol. The initial absorbance spectrum of the solution is recorded using a TECAN INFINITE MPLEX reader followed by the addition of 100mM of reducing agent sodium borohydride. A decrease in absorbance at 400 nm corresponding to a reduction of p-nitrophenol is monitored for the next ten minutes in kinetics mode at each ten second time interval. Similar catalytic reduction is performed using BSA@AuNCs in phase separated form, having 1mg/ml of nanocluster, 500mM sodium sulfate and 5%w/v PEG-6000 mixed with 100µM of p-nitrophenol. Further, we calculated the rate of reaction for BSA@AuNCs in dispersed and phase separated form, from the slope of the curve by fitting the data to the first-order decay kinetics equation (**equation 1**) using OriginPro 8.6 software.

$$-\ln\left(\frac{A}{A^{\circ}}\right) = kt \quad \text{..... equation 1}$$

(A-Absorbance value at certain time points, A°-Initial absorbance value, k- rate of reaction, t-time in seconds).

Peroxidase activity-

To check the peroxidase activity of BSA@AuNCs and BSA-$CuPO_4$ nanoflowers, oxidation of pyrogallol to purpurogallin is done in dispersed and in phase separated forms. The reaction mixture is having 1mg/ml of BSA@AuNCs and 20µl of nanoflowers of concentration 5µM separately and mixed with different concentrations of pyrogallol (100µM-1000µM) followed by addition of 0.1M H_2O_2. Production of purpurogallin is tracked by observing an increase in absorbance at 420 nm using a TECAN INFINITE MPLEX plate reader at kinetics mode. Reading is recorded at a time interval of one minute for a complete one hour. Next, the experiment is done using both the nanocomposites in a phase separated state with the same concentrations of pyrogallol as explained above with 500mM sodium sulfate and 5%w/v of PEG-6000 followed by the addition of 0.1M H_2O_2. Further, the rate of reaction at different pyrogallol substrate concentrations is plotted and the K_m and V_{max} of the reaction

are calculated after fitting the data in the Michaelis-Menten kinetics equation (**equation 2)** given below using GraphPad Prism 6 software for BSA@AuNCs in both the phases.

$$v = \frac{Vmax\,[S]}{Km+[S]} \quad \text{..... equation 2}$$

v- velocity of reaction, V_{max}- the maximum rate of reaction achieved by the system, [S]- Substrate concentration, K_m- Michaelis-Menten constant.

Peroxidase activity of prepared BSA@AuNCs is also checked against oxidation of another peroxidase substrate o-phenylenediamine to yellow-colored product diaminophenazine. Peroxidase assay is performed using 1mg/ml of nanoclusters solution with 0.2mM OPD and 1mM H_20_2. The formation of product DAP is tracked by recording absorbance and PL spectra of the reaction mixture in a steady-state kinetic assay of 30 minutes with 1 minute time interval. For PL spectra sample is excited at 400 nm and an increase in emission intensity of the product at 565 nm is tracked for continuous 30 minutes. Further, we performed the peroxidase kinetic assay after inducing liquid-liquid phase separation of the BSA@AuNCs using 500mM sodium sulphate and 5%w/v PEG-6000. We fitted the absorbance and fluorescence spectral data to calculate the rate of reaction in both conditions using the first- order kinetic equation represented as **equation 1** above.

Synthesis and phase separation of α-synuclein coated gold nanoparticles-

We purified the α-synuclein protein according to the protocol by Jain et al[29]. Overnight grown primary culture is transferred to the fresh media followed by the addition of 0.8mM IPTG and incubated at 37°C for 4 hours. Cells are harvested by centrifuging the culture at 8000 rpm for ten minutes. Pellet is resuspended in the lysis buffer and boiled at 90°C for 30 minutes. Lysed cells are centrifuged at 11,000rpm followed by the addition of 10% streptomycin sulfate and glacial acetic acid to the supernatant. Further, a saturated solution of ammonium sulphate is used to precipitate the protein. To synthesize α-syn AuNPs, we first synthesize the citrate capped gold nanoparticles using trisodium citrate as a reducing agent[30]. Gold chloride solution of 500µM concentration is heated to boil followed by the addition of 10µl of 5%w/v of trisodium citrate. Solution is continuously stirred for the next one hour till the color of the solution is changed to wine-red. Further, we incubated citrate-capped gold nanoparticles with 250µM of purified α-synuclein protein for 24 hours with continuous stirring at 4°C. The sample is centrifuged and repetitively washed with water. Further, we resuspend the pellet in 500µl of distilled water to perform further experiments. Conjugated protein concentration is calculated from the absorbance spectra of α-syn AuNPs. To phase separate α-syn AuNPs we incubated the α-syn AuNPs with 500mM sodium sulphate and 5% w/v of PEG-6000. We drop-casted the sample on a microscopic slide and observed the formation of liquid droplets using an upright fluorescence microscope OLYMPUS BX53 (OLYMPUS; USA).

Catalytic activity of α-synuclein coated gold nanoparticles -

We performed the oxidation and reduction reaction of aromatic compounds using α-synuclein coated gold nanoparticles. Reduction of p-nitrophenol to p-aminophenol is performed using 70µM of protein-coated gold nanoparticles with 50µM of PNP followed by the addition of 4mM of $NaBH_4$. A decrease in absorbance at 400 nm is noted in a kinetic cycle of 15 minutes with 30 second time interval. Oxidation of pyrogallol to purpurogallin is also performed using the same concentration of α-synuclein coated gold nanoparticles. The reaction is performed at different concentrations of pyrogallol ranging from 100µM-3mM in dispersed and phase separated states. The formation of purpurogallin is observed by recording an increase in absorbance corresponding to 420 nm. We calculated the K_m and V_{max} of the reaction after fitting the data in the Michaelis-Menten equation using GraphPad Prism software.

Disruption of liquid condensates-

Liquid condensates were disrupted using hexanediol. 10%w/v of hexanediol was added to the phase separated liquid condensates of BSA@AuNCs and imaged under a fluorescence microscope. Further reduction of p-nitrophenol was performed using BSA@AuNCs in dispersed, phase separated and hexanediol systems individually. The catalytic rate of reaction was calculated for each of the systems individually using the first-order decay kinetic equation **(equation 1)**.

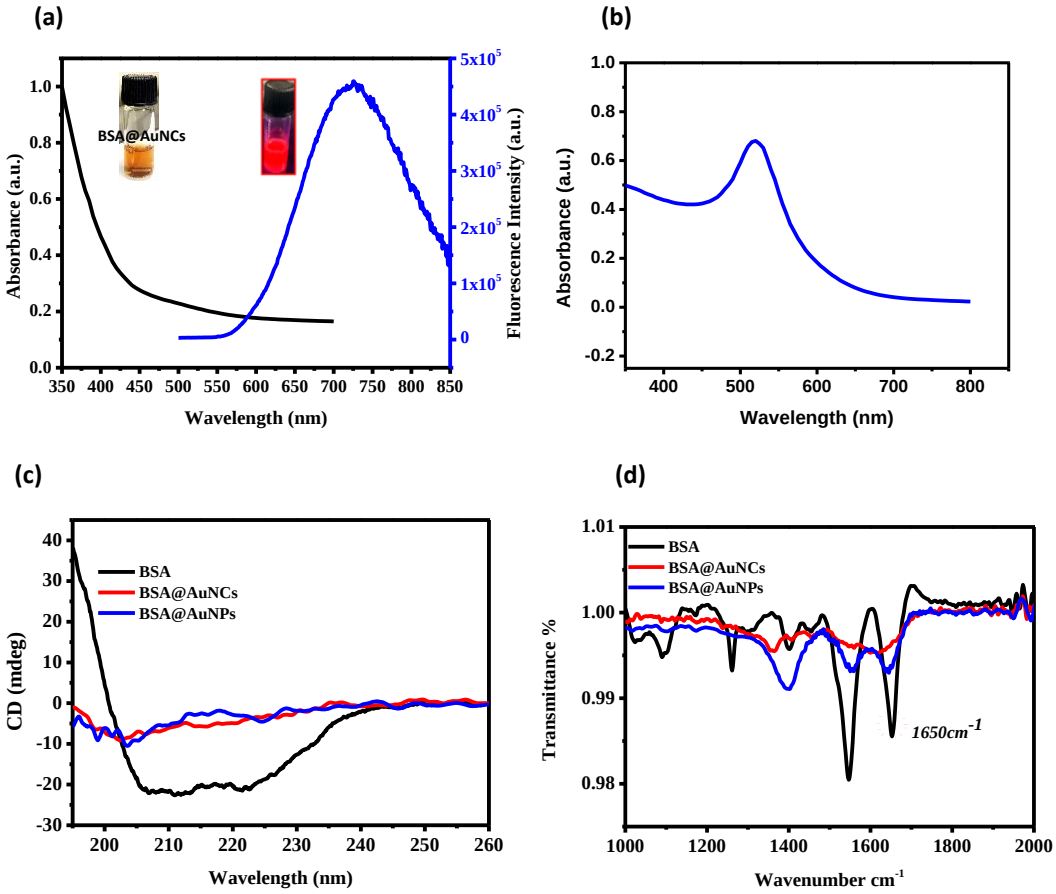

Figure S1: (a) Absorbance and fluorescence spectra (excitation at 450nm) of BSA@AuNCs. Inset shows the suspensions of BSA@AuNCs in stray light and under UV-lamp, (b) Absorbance spectra of BSA@AuNPs, (c) CD spectra of the native structure of BSA, BSA@AuNCs, and BSA@AuNPs showing a decrease in α-helix content of BSA in BSA@AuNCs and BSA@AuNPs, (d) FTIR spectra of BSA, BSA@AuNCs, and BSA@AuNPs showing the disappearance of peaks correspond to α-helix of BSA in BSA@AuNCs and BSA@AuNPs.

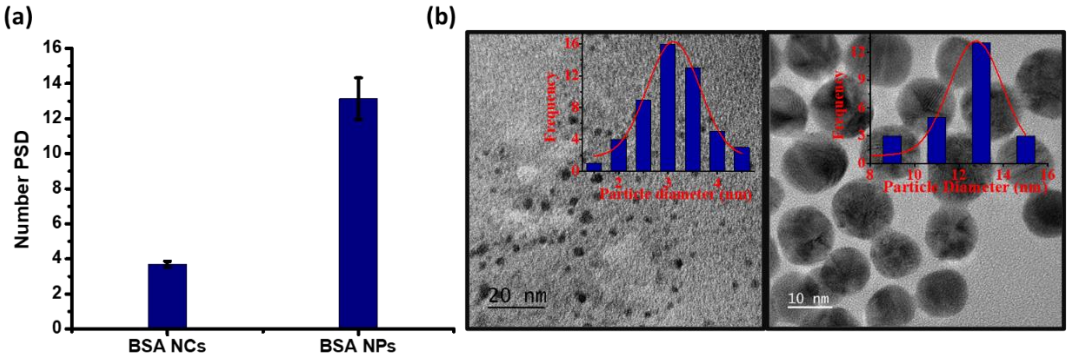

Figure S2: Size characterization of nanocomposite: (a) Number distribution of BSA@AuNCs and BSA@AuNPs; (b) TEM image of BSA@AuNCs and BSA@AuNPs, Inset shows the frequency distribution plot of the average size distribution of nanoclusters and nanoparticles: BSA@AuNCs-: 3-5 nm and BSA@AuNPs-:13-15nm.

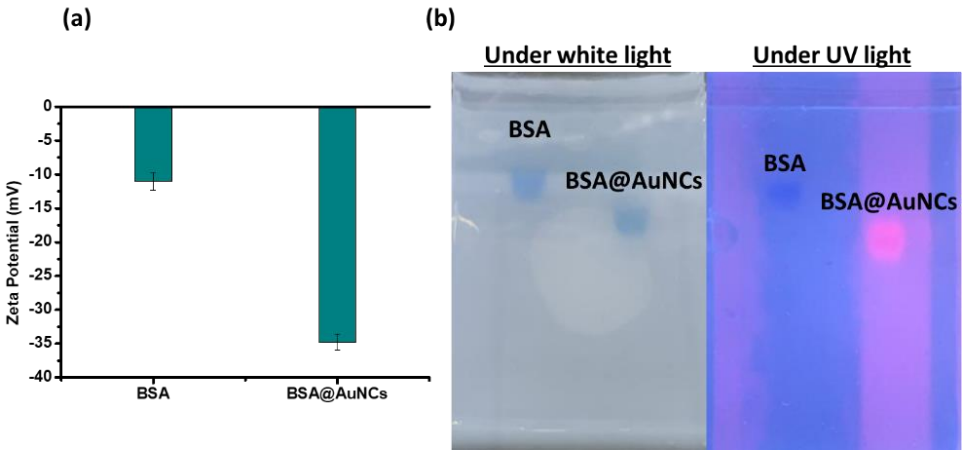

Figure S3: Evidence of BSA conjugation to nanoclusters: (a) Zeta potential of BSA and BSA@AuNCs; (b) Agarose gel showing bands for BSA and BSA conjugated nanoclusters, images have been taken under stray light and after irradiating with UV light.

Discussion: Wrapping of BSA around the gold nanoclusters shifts the zeta potential from -10mV to -35mV, which results in a difference in their electrophoretic mobility. **Fig. S3b** represents the band for BSA **(Lane1)** and BSA@AuNCs **(Lane2)**. As BSA@AuNCs are more negatively charged they are moving faster in comparison to the BSA alone. On irradiating UV light, we have seen a fluorescent band for BSA@AuNCs characteristic of BSA conjugated nanoclusters.

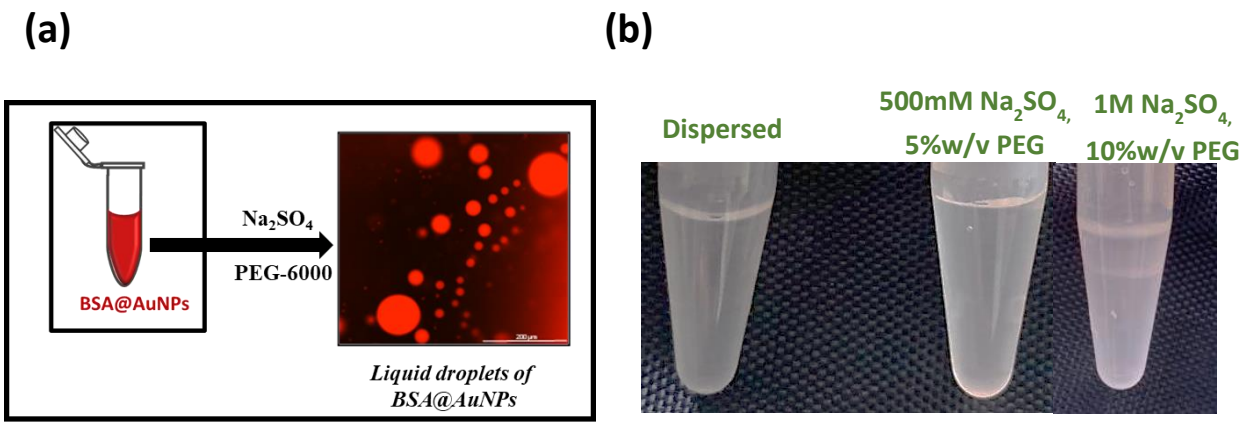

Figure S4: (a) Microscopic visualization of phase separated liquid droplets of BSA@AuNPs in presence of 500mM Na_2SO_4 and 5% w/v of PEG-6000, (b) macroscopic visualization of BSA@AuNPs on increasing salt concentration to 1M.

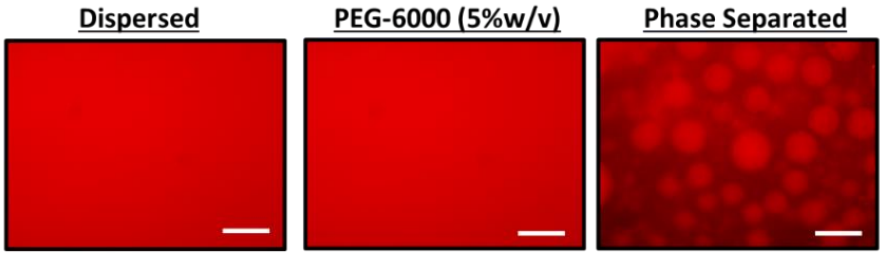

Figure S5: Fluorescence microscopy of texas red labelled BSA@AuNCs in dispersed, PEG-6000 (5%w/v) and phase separated condition.

Discussion: In this experiment, we checked the presence of solely PEG on the initiation of the phase separation process. We observed that solely PEG does not phase separate the nanoconjugate**.** A combination of salt and PEG is required to initiate the phase separation process.

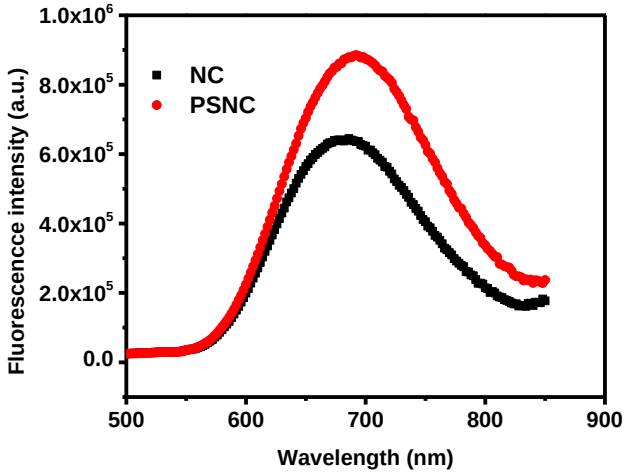

Figure S6: Fluorescence emission spectra of BSA@AuNCs (excitation-450nm) in dispersed (black line) and phase-separated liquid condensate form (Red line).

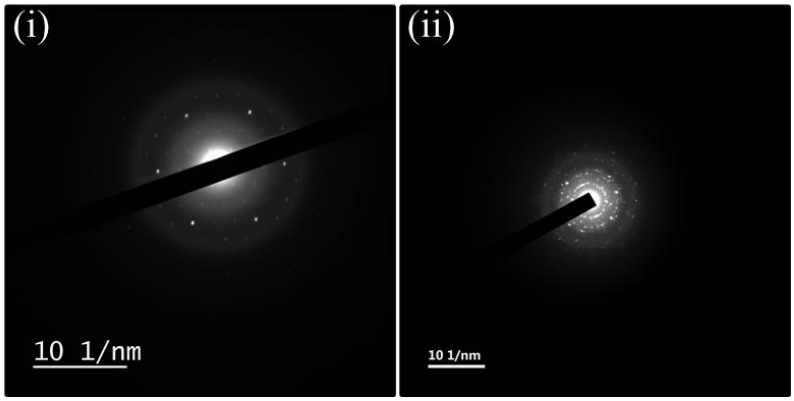

Figure S7: SAED pattern of (i) dispersed BSA@AuNCs and (ii) phase separated BSA@AuNCs.

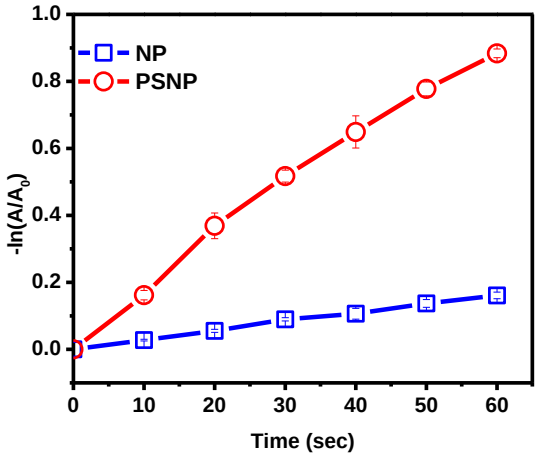

Figure S8: First order decay kinetic fit of reduction reaction of p-nitrophenol using BSA@AuNPs in dispersed (NP, blue line) and in phase separated condensate form (PSNP, red line).

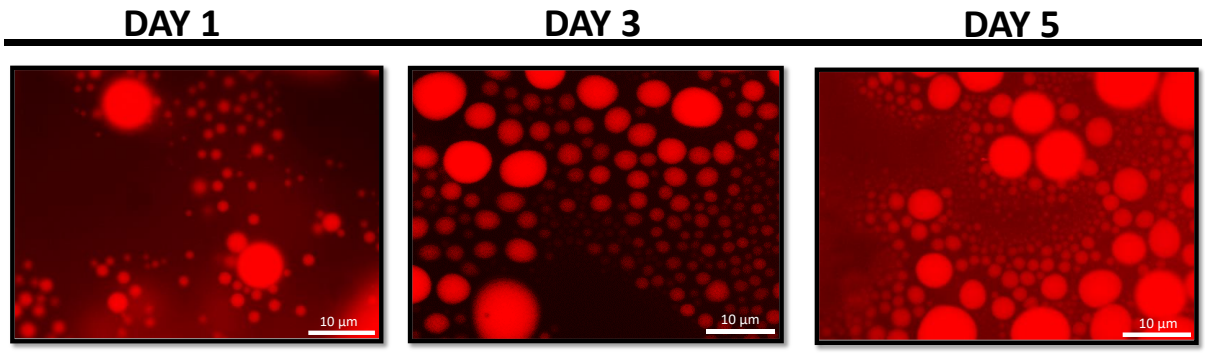

Figure S9: Day-dependent visualization of BSA@AuNCs liquid droplets, showing stable liquid droplet phases of BSA@AuNCs till five days of measurement.

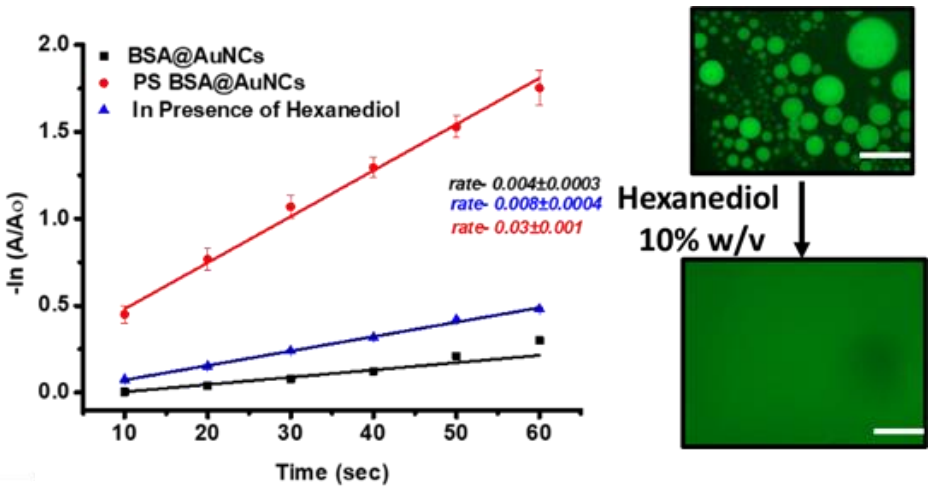

Figure S10: Disruption of molecular condensates: Fluorescence microscopic images of Alexa-labelled phase separated BSA@AuNCs before and after adding hexanediol, graph shows the decrease in the catalytic rate of reaction on adding hexanediol to the molecular condensates.

Discussion: The addition of 10%w/v hexanediol to the phase separated condensates of BSA@AuNCs dissolves the liquid condensates. Dissolution of condensates results in a decrease in the catalytic rate of reaction. This concludes that the phase separation process enhanced the catalytic rate of reaction.

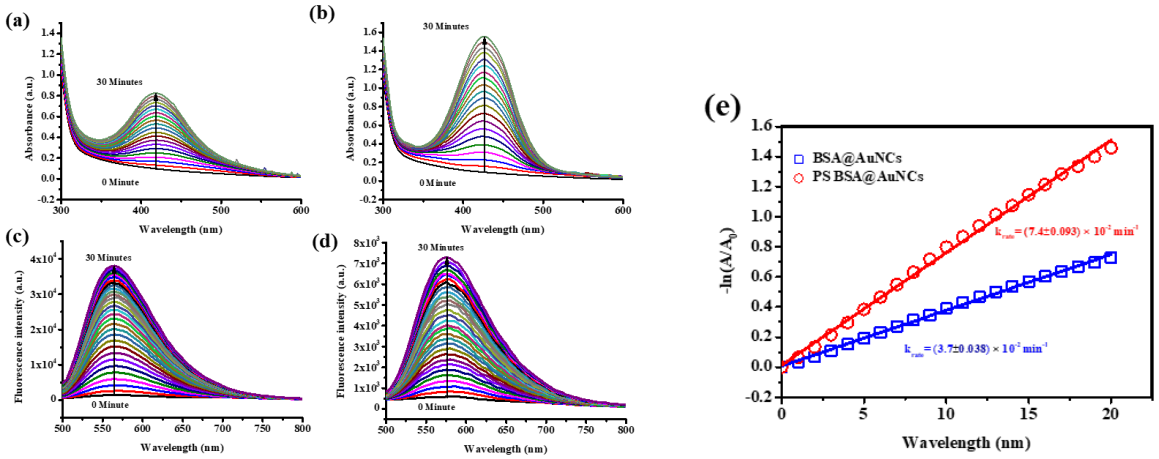

Figure S11: Increase in absorbance of product diaminophenazine (DAP) at 420nm with an increase in oxidation of substrate o-phenylenediamine (OPD) (a) dispersed BSA@AuNCs, (b) phase separated BSA@AuNCs; increase in emission intensity at 565nm upon 420nm excitation (c) dispersed BSA@AuNCs (d) phase separated BSA@AuNCs, (e) Fitted plot for Rate of reaction of DAP formation at 420 nm using first-order decay kinetic equation of BSA@AuNCs in dispersed (blue line) and phase separated form (red line).

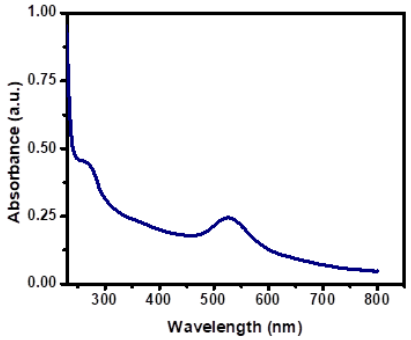

Figure S12: Absorbance spectra of α-synuclein coated citrate capped AuNPs.

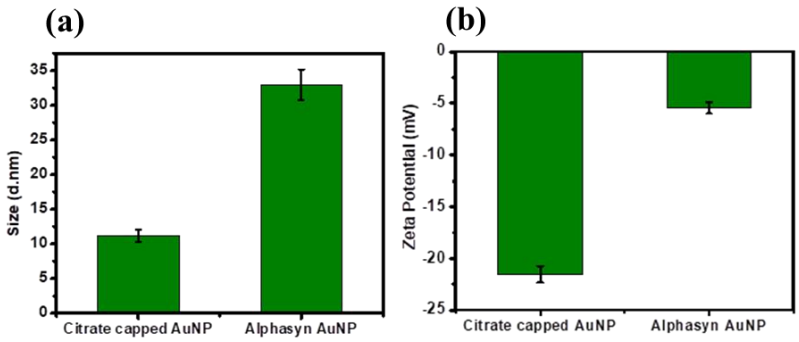

Figure S13: (a) Change in the hydrodynamic diameter of citrate capped AuNPs after conjugation with α-synuclein, (b) decrease in the zeta potential of citrate capped AuNPs due to interaction with positively charged N-terminal of α-synuclein protein.

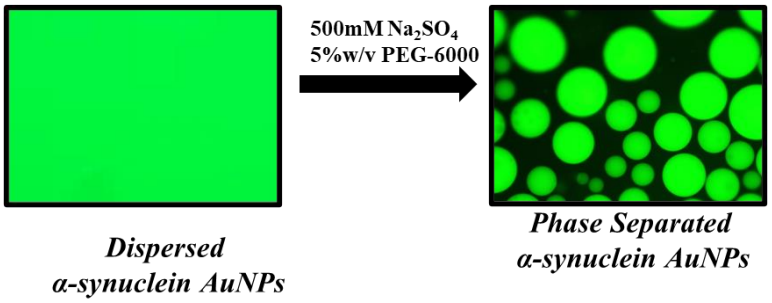

Figure S14: Microscopic visualization of liquid droplets of α-synuclein AuNPs in presence of 500mM Na_2SO_4 and 5%w/v PEG-6000.

Sample	K_m(μM)	V_{max} (Ms^{-1})
Dispersed α-syn AuNPs	3.18±0.66	0.01±0.001
Phase Separated α-syn AuNPs	1.18±0.18	0.02±0.001

Table S1 indicates the K_m and V_{max} values for peroxidase activity of α-syn AuNPs in dispersed solution and phase separated form.

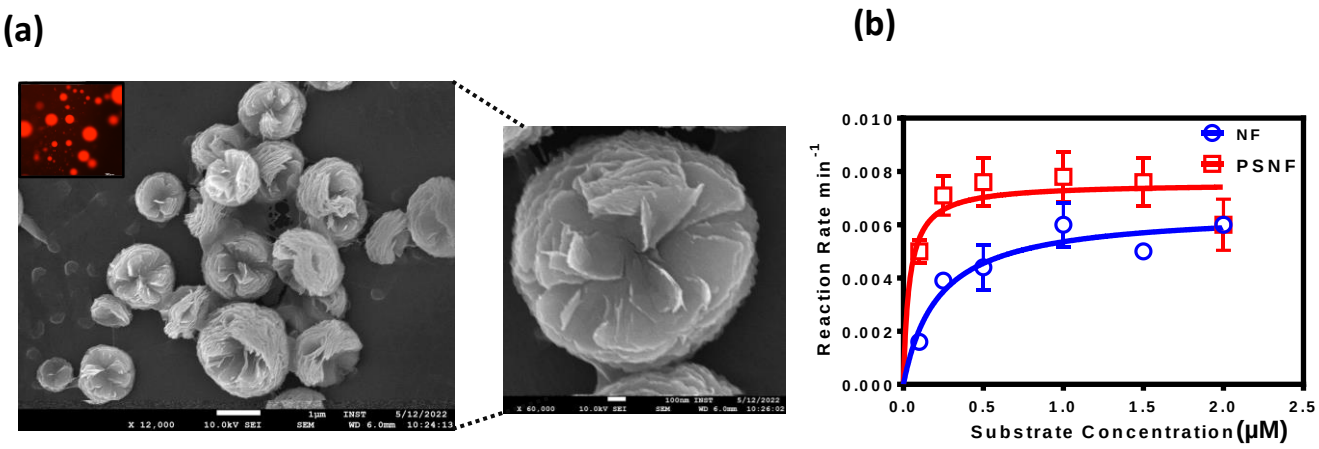

Figure S15: (a) FESEM image of BSA-$CuPO_4$ nanoflowers, inset shows the liquid-liquid phase separation of nanoflowers in presence of 500mM sodium sulphate and PEG-6000 (5% w/v); (b) oxidase activity of BSA-$CuPO_4$ nanoflowers for oxidation of pyrogallol to purpurogallin as a dispersed solution (blue line) and in phase separated form (red line). The graph represents the Michaelis-Menten Fit for the kinetics data for kinetic reaction of sixty minutes.

Table S2: The values for K_m and V_{max} of BSA-Copper phosphate Nanoflower and Phase separated Nanoflowers		
	K_m (µM)*	**V_{max} (Ms^{-1})***
Nanoflowers	**0.22±0.01**	**0.06±0.001**
Phase separated nanoflowers	**0.04±0.001**	**0.08±0.001**
A lower K_m in the case of phase separated nanoflowers indicates a higher affinity towards the substrate the comparable Vmax values in both cases indicate the phase separation does not alter the enzyme kinetic rate.		